Radial Distortion Measurement using Retinal Images of a Tunable Eye Model

Yuanxin Guan, Jim Schwiegerling, Travis William Sawyer, Florian Willomitzer
Wyant College of Optical Sciences, University of Arizona, Tucson, AZ, U.S.A.

Abstract: We demonstrate a first-generation system to measure the distortion value in the retinal images of an eye model with the presence of various degrees of ametropia. Our system can be used to examine the relation between lens-induced distortion and myopia progression in future research studies.

Keywords: visual optics, distortion measurement, refractive error, myopia progression, computational imaging, ophthalmology.

1. Introduction

Understanding myopia progression in the human eye is a research topic that has gained significant interest in the past decades. While the exact trigger for myopia progression is still unclear, experiments on animals have shown that myopic progression can be induced by mounting negative or positive lenses on the eye, even in the case of a severed optic nerve [1-4]. This astonishing result implies that lens-induced progression is not a perceptual artifact and ultimately gives rise to the question if a purely physical stimulus on the retina level may trigger this development. In this contribution, we demonstrate a system that allows us to measure distortion from retinal images of an artificial human eye model. Our system presents a first step towards answering the bigger question if myopia progression can be caused by lens-induced distortions on the retinal level.

2. Background and Contribution

In a previous work by our team [5], we simulated 1000 schematic eye models with a range of ametropia from $-20D$ to $+9D$, which suggested that the amount of radial distortion present at the retina surface is close to zero. However, inserting single vision spectacle lenses (SVLs) with correct prescriptions in front of these eye models creates a steep linear trend in radial distortion values (diopter vs. radial distortion), while inserting soft contact lenses (SCLs) generally creates a linear trend with lower slope. This simulation investigates SVLs and SCLs because they are two of the most common corrective schemes for refractive errors in the human eye [6] and are often used as control groups. The different amount of distortion introduced by different correction lenses prompts further investigation on the simulation to examine whether distortion plays a part in myopia progression.

A series of experiments are planned to build a novel optical device that measures distortion in the human eye with and without correction schemes. The experiments will aim to characterize the ocular distortion introduced by SVLs or other correction methods as a function of refractive errors. The results measured with an eye model will be used as a proof of concept before potentially moving into human trials. In this paper, we present a first step towards this direction: a first-generation benchtop system that is able to perform the described measurements. We will introduce the setup and show and explain a calibration method for future development of the device.

3. Experiment

The introduced prototype setup is built to capture the images of a grid pattern on the surface of the artificial retina of a tunable eye model before inserting correction schemes and calculate the radial distortion values from these retinal images. Our measurements performed in this contribution quantify the inherent radial distortion of the system with no correction scheme applied, which will be used as a calibration curve when measuring distortion with SVLs inserted in front of the eye model.

3.1 Experimental Setup

To capture retinal images, the optical system was designed to be double pass. A projector (Luma 350, Kodak) was used to project a 11 x 11 point-grid pattern into the ray path (see Fig. 1). After the first two lenses and a beam splitter, the beam path reaches an eye model which consists of two components: a tunable lens (EL-10-30, Optotune) and an artificial crude eye model [5]. The crude eye model has a focal length of 16mm which simulates the relaxed eye in air, and the tunable lens is used to simulate various levels of ametropia. It adds various powers between $+8.3\ D$ to $+20\ D$ to the crude eye model, so that the resulting system (tunable lens and crude eye model) can be tuned within a range of refractive error between $-8D$ and

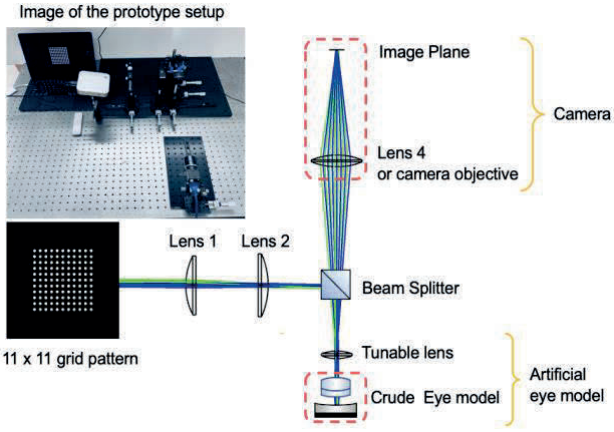

Fig.1. Schematic view and photo of the benchtop system (top left). The projector (white box in top left) emits the 11 x 11 point-grid pattern which forms an image on the retina and captured by the camera.

Paper presented at the 14th International Conference on Optics-Photonics Design & Fabrication, Tucson, July 10th-12th, 2024
Submitted: Feb. 14th 2024, Accepted: Apr. 12th 2024, Published in Abstract Digest: Aug. 15th, 2024 (https://doi.org/10.1117/12.3048202)

$+3.7D$. After forming an image at the modeled retina, composed of a curved fiber bundle that maps to a flat surface, the image is scattered and captured by a camera (BFS-U3-04S2C-C, Flir). The return path is simplified by selecting an appropriate camera objective lens. Some elements in the system shown in Fig. 1 are tilted slightly to avoid ghost reflections.

3.2 Measurements, Result and Discussion

Twenty-two images were taken with the tunable lens set to different powers and run through an image processing algorithm. The algorithm is used to find and record the centroids of the point-grid pattern. Since distortion is a cubic change in the field height, the four grid points that are in the closest vicinity of the center grid point are used to generate the reference grid. Radial distortion can then be calculated with the actual distance from the center to the diagonal corner of the captured grid and the predicted distance of the reference grid. The measurements are given from all four diagonal directions and then averaged for a more accurate result.

In our first experiment the tunable lens was tuned between $+14\,D$ to +18.5 D, which corresponds to a refractive error of the artificial eye between $-6.5D$ and $-2D$. Within this range, the captured images have barrel distortion and a visible change in the distortion while tuning the eye model. Also, a minor change in defocus was noticed in the system and was compensated by slightly tuning the objective lens of the camera. Three example images are shown in Figure 2 (a-c) with their processed states after the centroid-finding algorithm. The radial distortion in percentage was calculated and plotted with respect to the tunable lens diopter value which is shown in Figure 2 (d). The distortion is negative which agrees with barrel distortion. After capturing the "calibration measurements" and plotting the respective data in Fig. 2, we observe a nearly linear slope in the distortions caused by the optical system. After further refinements (e.g., accounting for the slight tilt visible in the data) we will use the captured curve to calibrate our system for further studies.

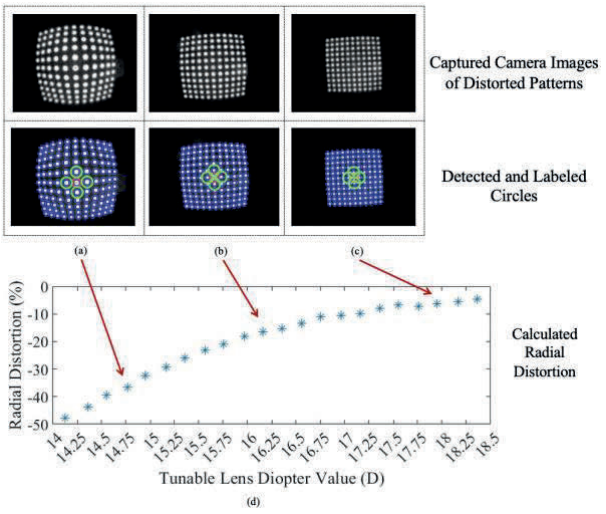

Fig.2. Example images (a-c) using three different add powers with the tunable lens along with the corresponding processed images. The plot (d) shows the relationship between the tunable lens add power and the radial distortion calculated from each image.

4. Future Work and Conclusion

While our prototype system is still at an early stage of its development, it has shown promising results and warrants further development. Optimization is needed to allow the system to utilize a larger range of powers with the tunable lens. Also, besides radial distortion, there are 18 coefficients from the second to the fourth order wavefront error that relates to distortion in a non-rotationally symmetric system [7]. It is important to map these coefficients for a more comprehensive understanding of the relation distortion may have with the myopia development. Therefore, additional algorithmic procedures can be performed on the captured grid points and the reference grid to account for the extra distortion coefficients. Future experiments will aim to quantify the additional ocular distortion introduced by inserting spectacle lenes with the correct prescriptions and compare these measurements with the afore mentioned simulation results.

5. Acknowledgment

The authors would like to thank and honor the late Dr. James Schwiegerling for conceiving the idea for this project and for his major contributions that made this project possible.

6. References

[1] Schaeffel, F., & Feldkaemper, M. (2015). *Animal models in myopia research*. Clinical and Experimental Optometry, 98(6), 507-517.

[2] Schaeffel, F., Glasser, A., & Howland, H. C. (1988). *Accommodation, refractive error and eye growth in chickens. Vision research*, 28(5), 639-657.

[3] Shaikh, A. W., Siegwart Jr, J. T., & Norton, T. T. (1999). *Effect of interrupted lens wear on compensation for a minus lens in tree shrews*. Optometry and vision science: official publication of the American Academy of Optometry, 76(5), 308-315.

[4] Hung, L. F., Crawford, M. L., & Smith, E. L. (1995). *Spectacle lenses alter eye growth and the refractive status of young monkeys*. Nature medicine, 1(8), 761-765.

[5] LaVilla, E. A. (2018). *Ocular Distortion Measurement and Relationship with Refractive Error* (Doctoral dissertation, The University of Arizona).

[6] Gwiazda J. (2009). *Treatment options for myopia.* Optometry and vision science: official publication of the American Academy of Optometry, 86(6), 624–628.

[7] Barakat, R., & Houston, A. (1966). The aberrations of non-rotationally symmetric systems and their diffraction effects. Optica Acta: International Journal of Optics, 13(1), 1-30.

Paper presented at the 14th International Conference on Optics-Photonics Design & Fabrication, Tucson, July 10th-12th, 2024
Submitted: Feb. 14th 2024, Accepted: Apr. 12th 2024, Published in Abstract Digest: Aug. 15th, 2024 (https://doi.org/10.1117/12.3048202)